Rune A.K. Bennedbaek, Chris V. Nielsen, Wenqi Zhang

Latest Developments in Simulation and Optimization of Resistance Welding Processes

Abstract: The paper summarizes the latest developments in numerical simulation and optimization of resistance welding as well as new developments in 3D simulation. Resistance welding simulation can be applied for the prediction of weld nugget sizes in various material combinations, and for the optimization and planning of welding process parameters. Weld quality can be modelled in terms of microstructural phase changes, resulting hardness distribution and strength under specified loading conditions. New developments for 3D simulation of complex joints allow for modelling strength testing and special effects such as shunting. Furthermore, projection welding often needs 3D simulation. 3D simulation of a new, lightweight, sandwich material is presented in the paper.

Keywords: resistance welding, numerical 3D simulation, welding parameters

DOI: 10.17729/ebis.2015.6/4

Introduction

Resistance welding is one of the most productive joining technologies widely applied in the automotive industry and other metal working industries. Introduction of new materials such as advanced high strength steels (AHSS) and aluminium alloys has led to more problems and difficulties in resistance welding. More welding tests are needed to understand the weldability of the new materials and to obtain optimal welding process parameters in order to improve weld quality and reduce expulsions (splashes). This has largely increased the cost of developments and time-to-market for launching new products.

Since the first commercialization of SORPAS® in 1999, numerical simulation of resistance welding has gained more and more industrial applications throughout the world [1-11]. The advantages of numerical simulations are obvious for saving time and reducing costs in product developments and process optimizations. This paper presents the latest developments on simulation and optimization of resistance welding with applications in weld planning, weld quality prediction and welding of new advanced lightweight materials.

Process simulation

The finite element method (FEM) is used in SORPAS® to build the numerical models for the simulation of resistance welding processes. The objective of process simulation is to study the weldability of new materials by predicting weld

Rune A.K. Bennedbaek, Wenqi Zhang – SWANTEC Software and Engineering ApS, DK-2800 Kgs. Lyngby, Denmark; Chris V. Nielsen – Department of Mechanical Engineering, Technical University of Denmark, DK-2800 Kgs. Lyngby, Denmark

results with specified materials, electrodes and welding process parameters. This is the fundamental function for more advanced functions such as optimization and welding process planning.

Automatic procedures have been developed for preparing input data, speeding up the simulations with more convenient graphical user interface and displaying weld results. After simulation, the dynamic process parameter curves can be displayed as functions of time, which include the process curves of voltage, current, power, resistance, force, displacement of electrode and evolution of the weld nugget size etc. The distributions of temperature, current, voltage, stress and strain in all materials can be visualized in animation throughout the welding process.

Figure 1 shows an example of the process simulation for spot welding of 1.0 mm mild steel sheets. Figure 1a shows the graphical user interface for preparing the input data with materials and welding process parameters. Figure 1b shows the report of simulation with the input conditions and the simulation results including a process parameter curve and the final weld nugget sizes.

Expulsion (or splash) is simulated by predicting the starting time of the splash during the welding process and also the intensity of splashes at three levels: low, medium and high. Figure 2a shows the dynamic resistance curve with the indication of the splash starting time and intensity. Figure 2b shows the final weld nugget with the indication of the splash intensity.

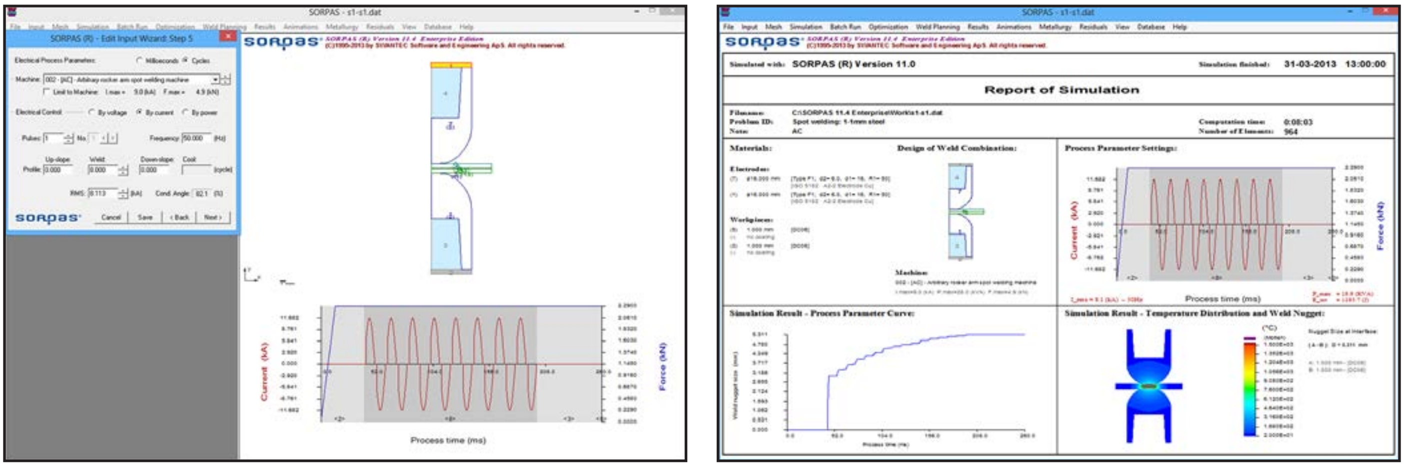

Fig. 1. Process simulation with SORPAS® showing input wizard for preparing input data of materials and welding process (left) and simulation report with input conditions and predicted weld results (right)

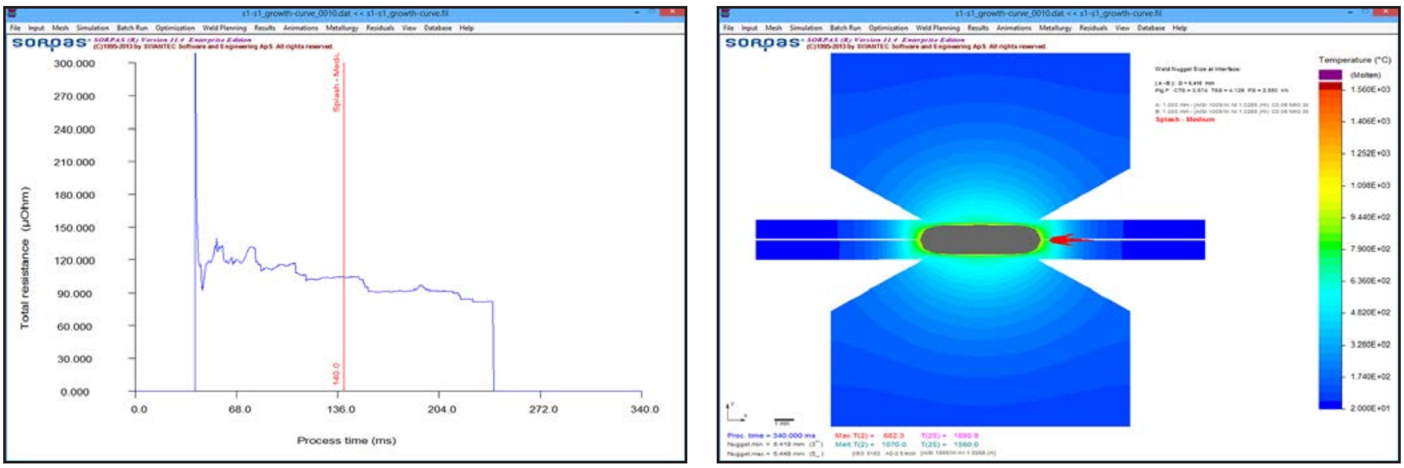

Fig. 2. Simulation of dynamic splash with prediction of the starting time and intensity of splash: process parameter curve with splash starting time and intensity in the welding process (left); final weld nugget sizes with indication of splash intensity (right).

Process optimization

Based on the results of process simulations, automated procedures have been developed for the optimization of the resistance welding process parameters. The weldability analyses and optimizations of resistance welding are presented in the international standard ISO 14327:2004 with two diagrams, including the weld growth curve and the weldability lobe. Both diagrams can be simulated automatically with SORPAS® with predicted expulsion (splash) limits and process window.

The weld growth curve can be produced by running a series of welding tests with increasing weld current and measuring the resulted weld nugget sizes. This is a tedious job with high costs of time and materials. It can now be simulated with an automated procedure for running simulations of all welds along the weld growth curve with the prediction of splashes.

The weldability lobes can be similarly simulated by running simulations of all welds in the specified ranges of weld current and weld force with the prediction of the welding process window. Two types of weldability lobes can be simulated with two varying process parameters. The first type is with varying weld current and time but constant weld force. The second type is with varying weld current and force but constant weld time.

Figure 3 shows the process optimizations for spot welding of 1.0 mm mild steel sheets. Figure 3a shows the simulated weld growth curve with weld nugget diameter as a function of weld current. It is seen that the weld nugget starts to form at a certain weld current and then grows with increasing weld current. The black (or square) points mean no weld or an undersized weld. The red (or triangular) points indicate expulsions (or splashes). The green (or round) points in the middle are good welds, which indicate the welding process window with the working range of weld current. Figure 3b shows the weldability lobe with current and weld force as the two varying parameters at a constant weld time. The black (or square) points are no weld or undersized welds. The red (or triangular) points are expulsion (splash) welds. The green (or round) points indicate good welds and the welding process window.

Weld planning automated for spot welding of steel and aluminium

After predicting the welding process window with the optimization procedures, a further demand of the industry is to determine the weld schedule specifications with optimal welding process parameters. The new function Weld Planning has been developed based on optimization procedures to predict the optimal welding parameters with specific current, force and time for a specific weld task. With the newly released SORPAS® 2D version 12, the weld planning works with a lot of improvements for spot

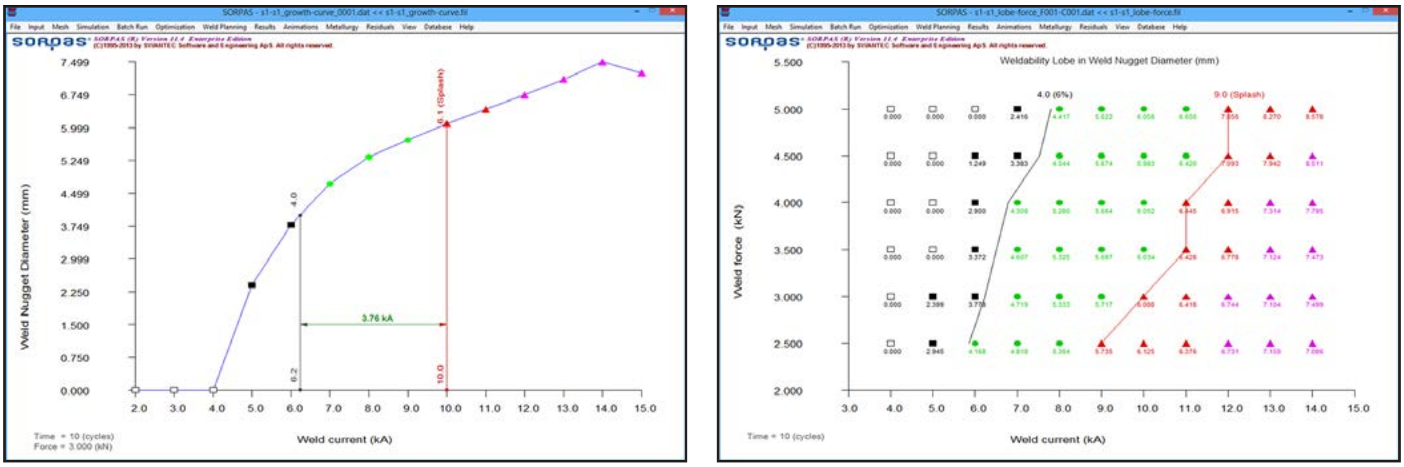

Fig. 3. Process optimizations with SORPAS® by means of weld growth curves with weld current range (left) and weldability lobes with weld process window (right)

welding of steels and also extended to work as well for spot welding of aluminium alloys.

Figure 4a shows the graphical user interface of the Weld Planning function for preparing the Weld Task Description (WTD) with information of the sheets, electrodes and welding machine. A special algorithm has been developed to automatically analyse the combination of sheet material and thickness, determine the weld force and weld time, and then obtain the welding process window. Thereby the optimal weld current, force and time can be obtained. Figure 4b shows the Weld Planning Report with the input data for the weld task description (WTD); the graphical display of the optimal welding process parameters; the Weld Schedule Specifications (WSS) with optimal weld current, force, weld time and hold time together with the welding process window; and the welding results obtained with the optimal welding process parameters.

Based on the simulated optimal welding process parameters, users can quickly determine the starting welding process parameters.

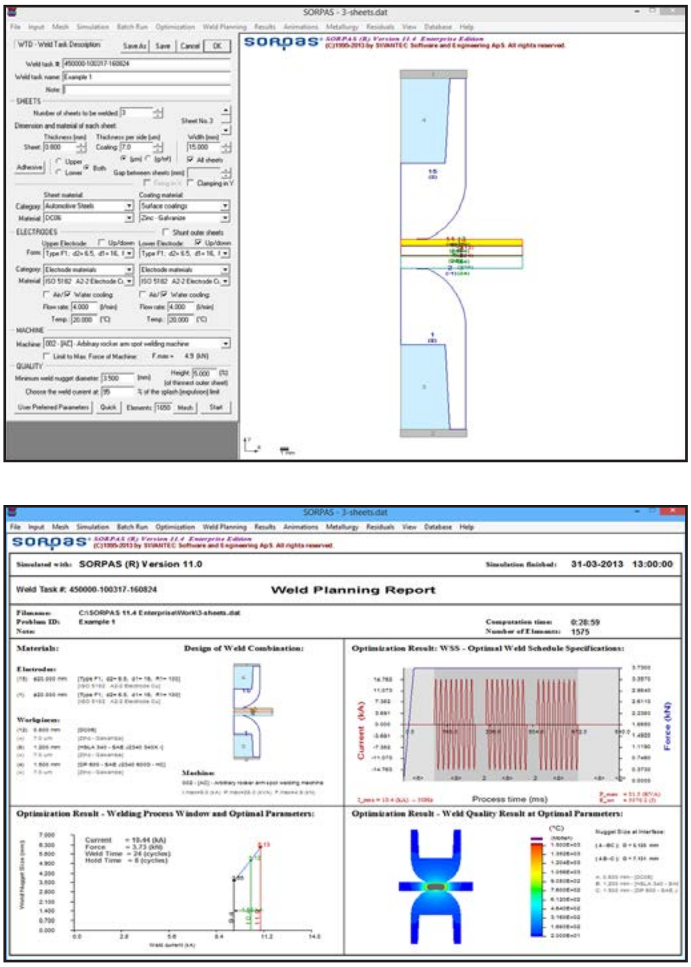

Fig. 4. Weld Planning for obtaining the optimal welding process parameters. Weld Task Description to define sheets, electrodes and welding machine (top); the predicted optimal process parameters, process window, and weld results (bottom)

Weld properties after welding

The weld properties, in terms of microstructural phase changes and the hardness distribution, are calculated in SORPAS® for typical automotive steel grades. Furthermore, in SORPAS® 3D, it is possible to simulate strength testing based on the predicted hardness distribution and thereby predict the strength of a weld under a giving loading condition.

During heating, the calculation of austenitization is based on the Ac1 and Ac3 temperatures independent from the heating rate. Full austenitization is assumed when the process peak temperature is above the Ac3 temperature; zero austenite formation is assumed when the process peak temperature is below the Ac1 temperature; and linear interpolation is applied in between the Ac1 and Ac3 temperatures. Transformation of the predicted austenite upon subsequent cooling is based on critical cooling rates in continuous cooling transformation (CTT) diagrams. Following the formulas presented by Blondeau et al. [12], the critical cooling rates for the formation of martensite, bainite and ferrite/pearlite are estimated by the chemical compositions. Formulas for the hardness of each phase are provided by Maynier et al. [13] with the dependency of chemical composition. The total hardness is predicted based on volume mixing of the hardness of each individual phase.

Figure 5a shows an example of the predicted hardness distribution in spot welding of two 1mm thick sheets. The upper sheet is a low carbon DC06 deep drawing steel and the lower sheet is a dual phase high strength steel DP600. The figure shows the hardness of the base material around the nugget and the hardness due to austenitization and the formation of subsequent phases during cooling in the weld nugget and in the heat affected zone (HAZ). The HAZ shows the difference between the two sheets. A large amount of martensite is formed in the DP600 steel with the resulting increase of hardness, while almost no martensite was formed in the HAZ of the DC06 where the hardness remained almost unchanged. In the nugget, volume mixing results in the formation of phases due to the mixed chemical composition. In this case some martensite was formed and an increase of hardness compared to both of the base materials. Figure 5b shows an example of cross-tension strength testing [14]. The simulation shows the localization of damage outside the nugget in agreement with the experimental observation of plug failure. Load-elongation curves for tensile-shear, cross-tension and peel strength testing are given in the references. Further details on the metallurgical changes, hardness prediction and damage implementation are given elsewhere [15].

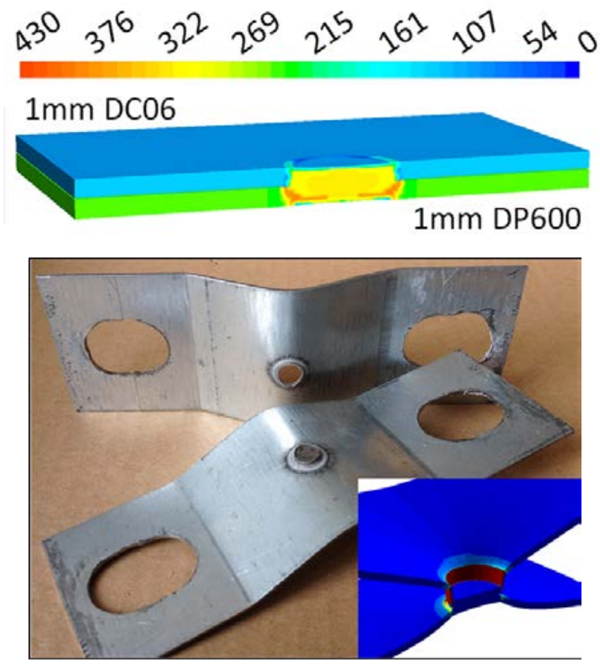

Fig. 5. Simulation of (a) hardness Vickers distribution in spot welded DC06-DP600 combination (top) and cross-tension strength testing of two DP600 steel sheets (bottom) [14]. The simulation shows the localization of damage in accordance with the experimentally observed full plug failure mode.

3D simulation of new, sandwich material

A new application of simulation by Sorpas® 3D is spot welding involving new, lightweight, sandwich materials such as Litecor®. For more details of the Litecor® sandwich material see [16-17]. Figure 6 shows an example of two DC06 sheets being spot welded to a centre layer of Litecor®, where an additional shunt tool is included in the setup in comparison to traditional spot welding. In the initial stage of the process, the current flows as schematically illustrated in Figure 7a through the outer sheets and the shunt tool without passing through the weld zone. This current flow results in heating and softening of the polymer layer in the Litecor® and in combination with the applied electrode force this leads to squeezing out of the polymer in the weld zone to reach metal-metal contact and a current flow as illustrated in Figure 7b. The current passing through the four metal layers produces a spot weld joining the three sheets.

Sagüés Tanco et al. [18] have presented experiments and simulations by Sorpas® 3D of the case outlined in Figures 6 and 7. Some of these results are presented as follows. The simulated current density before squeezing out the polymer (corresponding to Figure 7a) is shown in Figure 8a at a selected time step. It is visible how the current flows through the outer sheets and the shunt tool while not passing the polymer layer of the Litecor®. Figure 8b shows the current density during a selected time step

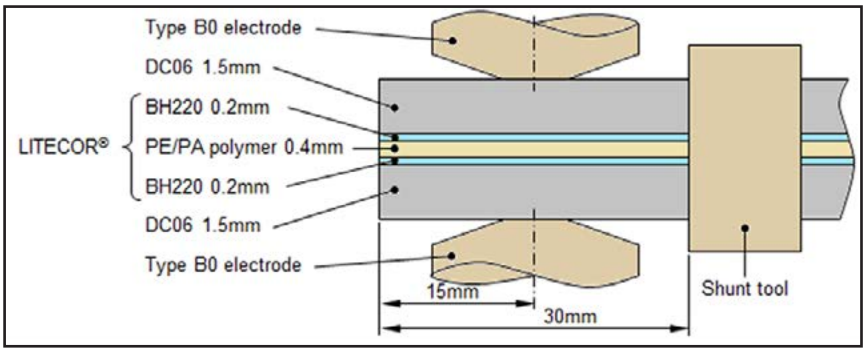

Fig. 6. Schematic illustration of spot welding of LITECOR® between two DC06 deep drawing steel sheets by utilization of a shunt tool to allow current flow before metal-metal contact in the weld position.

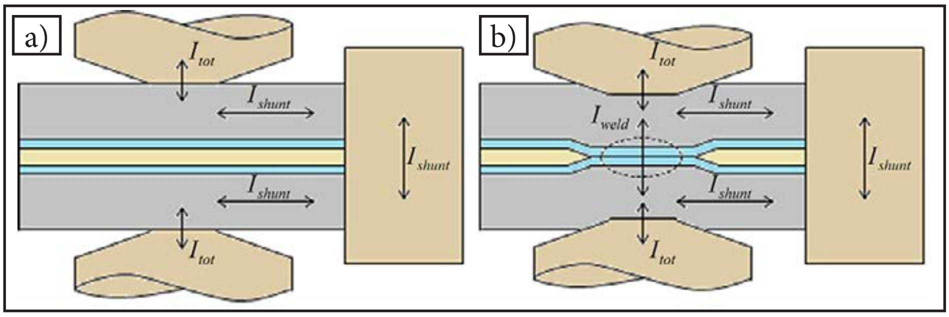

Fig. 7. Illustration of current flow (a) during initial heating and squeezing of the polymer to achieve metal-metal contact, and (b) during the actual welding stage.

after the polymer has been squeezed out and the current can pass through the spot to form a weld. Part of the current still passes the shunt tool. An example of a simulated weld nugget is presented in Figure 9a with comparison to the corresponding experiment in Figure 9b. The simulated nugget size measured at the interface between the DC06 sheet and the BH220 layer of the sandwich material was 5.05mm, which is in good agreement with the 5.11mm nugget size measured in the experiment. Further comparisons over the entire range of a weldability lobe can be found in [18].

Conclusions

Numerical simulation of resistance welding has been applied in industry for evaluations of the weldability of new materials and optimizations of welding process parameters. Two automated procedures have been developed for the optimization of welding process parameters with weld growth curves and weldability lobes. The new Weld Planning function is developed for predicting optimal welding process parameters to support welding production applications. The new developments in 3D simulations have made it possible to simulate more complex welding cases, whereas the 2D simulations are more suitable for simulation and optimization of spot welding and simple projection welding cases.

References

[1] Zhang W., Hallberg H., Bay N.: Finite Element Modelling of Spot Welding Similar and Dissimilar Metals. 7th Int. Conf. on Computer Technology in Welding, San Francisco, USA, pp. 364-373. 1997.

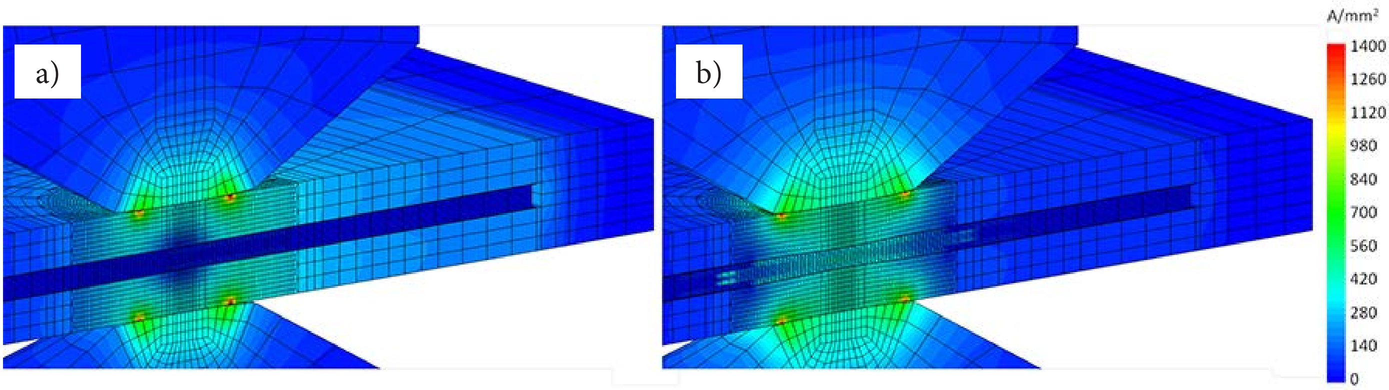

Fig. 8. Simulated current densities [18] corresponding to the schematic current flow in (a) Fig. 7a and in (b) Fig. 7b.

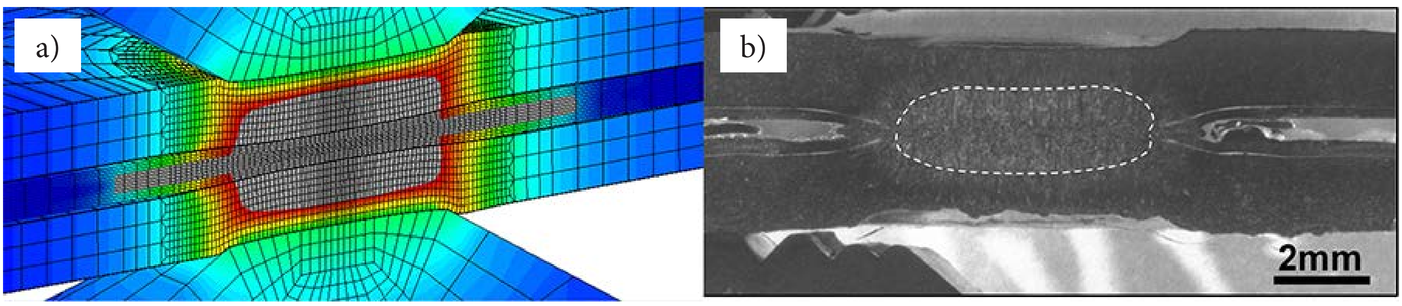

Fig. 9. Final weld nugget [18] by (a) simulation and (b) cross-sectional view of the corresponding experiment.

[2] Zhang W., Kristensen L.: Finite Element Modeling of Resistance Spot and Projection Welding Processes. The 9th Int. Conf. on Computer Technology in Welding, Detroit, Michigan, pp. 15-23. 1999.
[3] Zhang W.: Design and Implementation of Software for Resistance Welding Process Simulations. SAE 2003 Transactions: Journal of Materials and Manufacturing, Vol.112, No. 5, pp. 556-564. 2003.
http://dx.doi.org/10.4271/2003-01-0978
[4] A. Harthoej A., Pedersen K.R.: Analysis and Modeling of Microstructure and Hardness in Resistance Welding of Steels. B.Sc.-Thesis. Technical University of Denmark. 2008.
[5] Nielsen C.V., Friis K.S., Zhang W., Bay N.: Three-Sheet Spot Welding of Advanced High-Strength Steels. Welding Journal Research Supplement, Vol. 90 (2), pp. 32s-40s. 2011.
[6] Zhang W., Chergui A., Nielsen C.V.: Process Simulation of Resistance Weld Bonding and Automotive Light-weight Materials. Proceedings of the 7th International Seminar on Advances in Resistance Welding. Busan, Korea, pp. 67-75. 2012.
[7] Nielsen C.V., Chergui A.,Zhang W.: Single-sided sheet-to-tube spot welding investigated by 3D numerical simulations. Proceedings of the 7th International Seminar on Advances in Resistance Welding. Busan, Korea 2012.
[8] Nielsen C.V., Zhang W., Alves L.M., Bay N., Martins P.A.F.: Modeling of Thermo-Electro-Mechanical Manufacturing Processes with Applications in Metal Forming and Resistance Welding. Published by Springer. 2013.
http://dx.doi.org/10.1007/978-1-4471-4643-8_8
[9] Nielsen C. V., Zhang W., Perret W., Martins P.A.F., Bay N.: Three-dimensional simulations of resistance spot welding. Proceedings of the IMechE Part D: Journal of Automobile Engineering Vol. 229, No. 7, pp. 885–897. 2015.
http://dx.doi.org/10.1177/0954407014548740
[10] Nielsen C.V., Zhang W., Martins P.A.F., Bay N.: 3D numerical simulation of projection welding of square nuts to sheets. Journal of Materials Processing Technology, Vol. 215, pp. 171-180. 2015.
[11] http://www.swantec.com.
[12] Blondeau R., Maynier P., Dollet J., Vieillard-Baron B.: Prévision de la dureté, de la résistance et de la limite d'elasticité des aciers au carbone et faiblement alliés d'après leur composition et leur traitement thermique. Mémoires Scientifiques Revue Métallurgie, pp. 759-769. 1975.
[13] Maynier P., Jungmann B., Dollet J.: Creusot-Loire system for the prediction of the mechanical properties of low alloy steel products. Hardenability Concepts with Applications to Steels. The Metallurgical Society of AIME Heat Treatment Committee / American Society for Metals Activity on Phase Transformations, pp. 518-545. 1978.
[14] Nielsen C.V., Bennedbæk R.A.K., Larsen M.B., Bay N., Chergui A., Zhang W., Martins P.A.F.: Experimental and Simulated Strength of Spot Welds. The 8th International Seminar on Advances in Resistance Welding, Baveno, Italy, pp.161-172. 2014.
[15] Nielsen C.V., Martins P.A.F., Zhang W., Bay N.: Numerical methods in simulation of resistance welding. VI International Conference on Computational Methods for Coupled Problems in Science and Engineering, pp. 322-333. 2015.
[16] Hoffmann O.: Environment oriented light weight design in steel. Ökologischer Leichtbau in Stahl, Hannovermesse Werkstoff-Forum, Hannover, Germany. 2012.
[17] Hoffmann O.: Steel lightweight materials and design for environmentally friendly mobility, Industrial Technologies 2012 integrating nano, materials and production. Aarhus, Denmark. 2012.
[18] Sagüés Tanco J., Nielsen C.V., Chergui A., Zhang W., Bay N.: Weld nugget formation in resistance spot welding of new lightweight sandwich material. International Journal of Advanced Manufacturing
http://dx.doi.org/10.1007/s00170-015-7108-0